# A Restricted Repertoire of De Novo Mutations in ITPR1 Cause Gillespie Syndrome with Evidence for Dominant-Negative Effect

# A Restricted Repertoire of *De Novo* Mutations in *ITPR1* Cause Gillespie Syndrome with Evidence for Dominant Negative Effect

Meriel McEntagart[1§], Kathleen A Williamson[2§], Jacqueline K Rainger[2], Ann Wheeler[2], Anne Seawright[2], Elfride De Baere[9], Hannah Verdin[9], L. Therese Bergendahl[2], Alan Quigley[18], Joe Rainger[2,3], Abhijit Dixit[8], Ajoy Sarkar[8], Eduardo López Laso[13], Rocio Sanchez-Carpintero[14], Jesus Barrio[20], Pierre Bitoun[4], Trine Prescott[5], Ruth Riise[6], Shane McKee[7], Jackie Cook[10], Lisa McKie, Berten Ceulemans[21], Françoise Meire[22], I Karen Temple[11], Fabienne Prieur[12], Jonathan Williams[17], Penny Clouston[17], Andrea H. Németh[19], Siddharth Banka[16], Hemant Bengani[2], Mark Handley[2], Elisabeth Freyer[2], Allyson Ross[2], DDD study[15], Veronica van Heyningen[2], Joseph A Marsh[2#], Frances Elmslie[1#], David R FitzPatrick[2#]

1.Medical Genetics, St George's University Hospitals NHS Foundation Trust, Cranmer Terrace, London, SW17 0RE, UK

2. MRC Human Genetics Unit, IGMM, University of Edinburgh, Western General Hospital, Edinburgh, EH4 2XU, UK

3. Roslin Institute, University of Edinburgh, Easter Bush, Midlothian, EH25 9RG, UK

4. Service de pédiatrie, CHU Paris Seine-Saint-Denis - Hôpital Jean Verdier Avenue du 14 juillet 93140 Bondy, France

5. Department of Medical Genetics, Oslo University Hospital, 0424 Oslo, Norway

6. Department of Ophthalmology, Innland Hospital, Elverum, Norway

7. Northern Ireland Regional Genetics Service, Belfast City Hospital, Belfast, BT9 7AB, UK

8. Clinical Genetics, Nottingham City Hospital, Hucknall Road, Nottingham, NG5 1PB, UK

9. Center for Medical Genetics Ghent (CMGG), Ghent University Hospital, Medical Research Building (MRB), 1st floor, room 110.029, De Pintelaan 185, B-9000 Ghent, Belgium

10. Sheffield Clinical Genetics Service, Sheffield Children's Hospital, Western Bank, Sheffield, S10 2TH, UK

11. Human Development and Health Academic Unit, University Hospital Southampton, Tremona Road, University of Southampton, SO16 6YD, UK

12. Service Génétique, Plateau de biologie, CHU Saint Etienne, 42055 Saint Etienne cedex 2, France

13. Pediatric Neurology Unit, Department of Pediatrics, Reina Sofia University Hospital, Av. Menéndez Pidal s/n, 14004 Córdoba, Spain

14. Paediatric Neurology, Unit, Department of Paediatrics, Clinica Universidad de Navarra, Pamplona, Spain

15. DDD Study, Wellcome Trust Sanger Institute, Hinxton, Cambridge, CB10 1SA, UK

16. Manchester Centre for Genomic Medicine, University of Manchester, St. Mary's Hospital, Oxford Road, Manchester, M13 9WL, UK

17. Oxford University Hospitals NHS Trust, Oxford Medical Genetics Laboratories, The Churchill Hospital, Old Road, Headington, Oxford, OX3 7LE, UK

18. Department of Radiology, Royal Hospital for Sick Children, Edinburgh, EH9 1LF, UK

19. Nuffield Department of Clinical Neurosciences, University of Oxford, OX3 7LJ, UK

20. Department of Ophthalmology, Clinica Universidad de Navarra, Pamplona, Spain

21. Department of Neurology-Pediatric Neurology, University and University Hospital Antwerp, Antwerp, 2650, Belgium

22. Department of Ophthalmology, Queen Fabiola Children's University Hospital, 1020 Brussels, Belgium

§ These authors contributed equally to this work

# These authors contributed equally to this work

Address for correspondence:

David R FitzPatrick, MRC Human Genetics Unit, IGMM, University of Edinburgh, Western General Hospital, Edinburgh EH4 2XU, UK

## Abstract

**Gillespie syndrome (GS) is characterized by bilateral iris hypoplasia, congenital hypotonia, non-progressive ataxia and progressive cerebellar atrophy. Trio-based exome sequencing identified *de novo* mutations in *ITPR1* in three unrelated individuals with GS recruited to the Deciphering Developmental Disorders study. Whole exome or targeted sequence analysis identified plausible disease-causing *ITPR1* mutations in 10/10 additional GS individuals. These ultra-rare protein-altering variants affected only three residues in ITPR1; Glu2094 missense (1 *de novo*, 1 co-segregating), Gly2539 missense (5 *de novo*, 1 inheritance uncertain) and Lys2596 in-frame deletion (4 *de novo*). No clinical or radiological differences were evident between individuals with different mutations. *ITPR1* encodes an inositol 1, 4, 5-triphosphate-responsive calcium channel. The homo-tetrameric structure has been solved using cryoelectron microscopy. Using estimations of the degree of structural change induced by known recessive and dominant negative mutations in other disease-associated multimeric channels we developed a generalizable computational approach to indicate the likely mutational mechanism. This analysis supports a dominant negative mechanism for GS variants in ITPR1. In GS-derived lymphoblastoid cell lines (LCLs) the proportion of ITPR1-positive cells using immunofluorescence was significantly higher in mutant than control LCLs, consistent with an abnormality of nuclear calcium signaling feedback control. Super-resolution imaging supports the existence of an ITPR1-lined nucleoplasmic reticulum. Mice with *Itpr1* heterozygous null mutations showed no major iris defects. Purkinje cells of the cerebellum appear to be the most sensitive to impaired ITPR1 function in humans. Iris hypoplasia is likely to result from either complete loss of ITPR1 activity or structure-specific disruption of multimeric interactions.**

Key Words: iris; aniridia; cerebellar ataxia; cerebellar vermis; cerebellar hypoplasia; ITPR1; calcium; inositol triphosphate; ACTA2

## Report

Ida Mann in her classic 1925 paper on the development of the iris in human embryos and fetuses[1] describes four major morphological stages. From 28-49 gestational days (GD) there is formation of the annular irido-hyaloid vessel at the distal rim of the optic cup, coincident with the apposition of the optic fissure and appearance of the lens placode. Between 50-77 GD, following the separation of the lens vesicle, the "mesodermal" iris appears as a thin layer distal to the lens, the central regions of which is known as the pupillary membrane. This layer is contiguous with the peri-ocular mesenchyme and the mesenchyme surrounding the hyaloid vessels. From 78-84 GD the ectodermal iris appears as a separate outgrowth from the tip of the optic cup coinciding with the disappearance of the irido-hyaloid vessels. The final stage, from 85-175GD, involves growth of the ectodermal iris, the outer layer of which is contiguous with the future retinal pigment epithelium and the inner layer with the neural retina. Both layers of the ectodermal iris eventually pigment. The sphincter muscles appear to develop from cells of the distal outer layer supplied by radial vessels from the mesodermal iris. The dilator musculature develops as a thin layer growing radially on the surface on the outer layer of the ectodermal iris.

The best-studied malformation of the iris is complete aniridia (MIM 106210) [2] with more than 90% of cases caused by heterozygous loss-of-function (LOF) mutations in the paired- and homeo-domain containing transcription factor *PAX6* (MIM 607108). *PAX6*-associated aniridia is, however, a pan-ocular disease typified by foveal hypoplasia, cataracts and progressive corneal opacification in addition to the iris anomaly [3]. Extraocular disease is rare in *PAX6*-associated aniridia although structural brain anomalies and other sensory impairments have been identified [4]. Apparently isolated aniridia has also been reported in association with heterozygous LOF mutations in *FOXC1* (MIM 601090) [5, 6] and *PITX2* (MIM 601542) [7] although these loci are more commonly associated with anterior segment dysgenesis (MIM 602482) [8]. Syndromic forms of aniridia have been described, the best known of which is WAGR (Wilms tumour, aniridia, genital malformations, intellectual disability (retardation); MIM 194072) resulting from a contiguous gene defect encompassing *PAX6* and *WT1* (MIM 607102) [9]. The other well-known syndromic form of aniridia is Gillespie syndrome (MIM 206700). Aniridia is, however, an incorrect description of iris malformation in

Gillespie syndrome, which is a characteristic form of iris hypoplasia with “scalloping“ of the pupillary edge. Gillespie syndrome typically presents as fixed dilated pupils in affected infants. Iridolenticular strands can be seen at regular intervals (Figure 1B) as can other remnants of the pupillary membrane. From the description of the embryology given above the iris defect in Gillespie syndrome would thus be consistent with a failure of development or maintenance of the sphincter musculature and the associated stroma. The eye in Gillespie syndrome can be further distinguished from *PAX6*-related disease by the absence of foveal hypoplasia and corneal opacification. The key extra-ocular features of Gillespie syndrome are congenital hypotonia, non-progressive cerebellar hypoplasia and ataxia (Figure 1B-D) and variable, usually mild, neurocognitive impairment. The inheritance of Gillespie syndrome has been considered heterogeneous with both autosomal dominant and autosomal recessive inheritance being postulated on the basis of convincing patterns in individual families [10, 11]. The clinical features of 13 affected individuals with a confident clinical diagnosis of Gillespie syndrome who were used in the molecular studies reported below are summarized in Table 1. We reviewed the available neuroimaging of each case, which showed that the cerebellar vermis atrophy is present early and is progressive particularly in the first five years of life (Figure 1B-D). The atrophy mainly affected the superior vermis progressing to involve the superior cerebellar hemispheres more than the inferior aspects. Abnormal periventricular increased T2/FLAIR white matter signal was seen adjacent to the frontal horns on all examinations and older patients also had scattered foci of increased T2/FLAIR signal in the white matter, mainly frontally. Until now the molecular basis of Gillespie syndrome was not known with causative mutations in *PAX6, FOXC1* and *PITX2* having been excluded in many reported cases [12].

Deciphering Developmental Disorders (DDD) is a UK and Ireland-wide project that aims to use whole exome sequencing to identify the cause of previously unexplained severe and extreme phenotypes which plausibly have their genesis in embryogenesis or early fetal brain development [13]. The study has UK Research Ethics Committee approval (10/H0305/83, granted by the Cambridge South REC, and GEN/284/12 granted by the Republic of Ireland REC) with written consent being obtained from all participating families. To date 13936 probands have been recruited with DNA samples available in the majority from the affected

individual and both parents (trios). Three individuals have been recruited to DDD with a clinical diagnosis of Gillespie syndrome (261348, 263220, 272179; Figure 1A) and these were whole exome sequenced as part of the first 4294 trios. The technical and analytical details of the trio exome analysis used in DDD have been previously reported [14-16]. Briefly fragmented genomic DNA was the substrate for targeted pull-down using a custom Agilent SureSelect 55MB Exome Plus and 75-base paired-end sequenced on Illumina HiSeq. Alignment was performed using Burrows-Wheeler Aligner (BWA; version 0.59) and realignment around indels using GATK. Putative *de novo* mutations were identified from exome data using DeNovoGear software [17]. The functional consequence of each variant was assessed using the most severe consequence from Ensembl Variant Effect Predictor (VEP) [18]. Plausibly pathogenic mutations in known developmental disorders were identified by filtering by gene and allelic requirement using the DDG2P database combined with the minor allele frequencies as described [16]. Using this approach each of the Gillespie syndrome cases in DDD was found to carry a single plausible pathogenic variant, which was a *de novo* protein-altering mutation in *ITPR1* (MIM 147265). Two of these individuals (261348 & 263220) had different heterozygous mutations affecting the same reference base (261348 chr3 g.4856205G>C; 263220 chr3 g.4856205G>A hg19) which is predicted to result in an identical change in the open reading frame (p.Gly2539Arg). The latter of these genomic mutations (3:4856205G>A) is recorded in 1/120716 (0.000008284) alleles in the ExAC database in an individual of recent African decent, although the inheritance or any associated phenotype of the carrier is not available. Individual 272179 had a heterozygous in-frame deletion of a single codon (chr3 g.4856866-4856868delAAG; p.Lys2596del). The BAM and VCF files from the first 4294 trios in the DDD project are available via the European Genome-Phenome Archive (EGA). All residue numbering uses reference sequence NP_001161744.1 (Q14643-2; ENSP00000306253.8), which represents ITPR1 isoform 2 with a total of 2743 amino acids and lacking a 15 amino acid insertion at Asp321. The *de novo* status of each of these variants was confirmed using an independent sequencing technology (Sanger or Illumina MiSeq). On review of the exome data no other plausibly pathogenic variant could be identified on the second allele in each of the three DDD cases.

Following identification of the *de novo ITPR1* mutations in the DDD cases we reviewed whole exome sequences that had been independently generated on a previously reported [19, 20] mother (SVP) and daughter (SW) with Gillespie syndrome. The exome capture had been performed using the SureSelectXT Human All Exon V5+UTRs kit (Agilent) followed by 150-base paired-end sequencing on a NextSeq 500 (Illumina). The CLC Genomics Workbench version 7.5 (Aarhus, Denmark) was used for read mapping against GRCh37/hg19, followed by duplicate read removal and coverage analysis for all regions enriched with the SureSelect XT exome kit. Approximately 98% of the target regions were covered in both patients. A read depth of at least 10x was obtained for 80.26% and 90.75% of the SureSelect target regions in both affected individuals, respectively. Finally, quality-based variant calling and annotation was performed and the resulting variant lists were exported for filtering. SVP and SW shared a single, heterozygous, ultra-rare missense mutation (not present in ExAC or 1000 genomes data) in *ITPR1* (chr3 g.4821268A>G; p.Glu2094Gly) (Supplemental Data). This study was conducted following the tenets of Helsinki, and written informed consent was obtained from the participating family.

Eight additional unrelated cases of Gillespie syndrome were identified via the eye malformation cohort held in the MRC Human Genetics Unit (MRC HGU) at the University of Edinburgh, a study approved by the UK Multiregional Ethics Committee (Reference: 06/MRE00/76) with written informed consent obtained from the participating families. Whole exome sequencing was available on one of these individuals (1388_1388) which, on review, was found to show a heterozygous mutation in *ITPR1* identical to the chr3 g.4856866-4856868delAAG; p,Lys2596del allele mentioned above. This mutation was subsequently shown to have occurred as a *de novo* mutation in this individual. No other plausible disease-causing mutations were identified in *ITPR1* from these exome analyses. Targeted re-sequencing was performed in the seven other individuals with a confident clinical diagnosis of Gillespie syndrome. Six exons of *ITPR1* were selected - coding exons 46 and 52 to 56, which encode the region spanning Glu2094 and the entire calcium ion channel domain, respectively (Table S2). This revealed heterozygous mutations in all seven affected individuals; 4/7 c.7615G>A p.Gly2539Arg, 2/7 c.7786_7788delAAG p.Lys2596del and 1/7 (chr3 g.4821267G>C; p.Glu2094Gln) (Figure 1A). In 6/7 of these individuals the mutation was not

present in DNA from the mother and father (all clinically unaffected) and biological relationships were confirmed using highly informative genetic markers suggesting that the mutations had occurred *de novo* in the affected individual. In 2018_2018 the mutation was not present in the unaffected mother but the father's DNA sample was not available for analysis. A separate cohort of 173 individuals with non-syndromic aniridia and with no mutation in *PAX6* detected, were screened for mutations in *ITPR1* using the targeted resequencing amplicons. No plausible disease-causing mutations were identified, suggesting that *ITPR1* mutations are specific for iris hypoplasia associated with Gillespie syndrome and that this locus does not contribute to other forms of aniridia. Thus all thirteen affected individuals with a clinical diagnosis of Gillespie syndrome that were available to us for study were found to have ultra-rare protein altering mutations affecting only three residues in ITPR1, with at least ten of these mutations having occurred *de novo*.

*ITPR1* encodes a calcium-release channel that is inositol 1,4,5-trisphosphate ($IP_3$)-responsive. Heterozygous LOF mutations, mostly deletions encompassing *ITPR1,* have been identified in spinocerebellar ataxia type 15 (SCA15; MIM 606658). SCA15 is characterized by very slowly progressive autosomal dominant cerebellar ataxia and cerebellar atrophy [21-26]. Haploinsufficiency for *ITPR1* accounted for 2% of dominant ataxia in a screen of a large series of well-characterized families with the age of onset in the affected individuals with *ITPR1* deletions in this series being between 18-66 years [23]. Earlier onset *ITPR1*-associated cerebellar disease has been reported. In two families with a congenital, non-progressive spinocerebellar ataxia (SCA29; MIM 117360) the disease was found to co-segregate with a different ultra-rare *ITPR1* missense mutation in each family (encoding c.1759A>G; p.Asn587Asp and c.4639G>A; p.Val1547Met: These and all subsequent numbering converted to NP_001161744.1 (Q14643-2, ENSP00000306253.8) with pathogenicity scores for all variants provided in Table S3) [27]. Another multigeneration family with c,4639G>A; p.Val1547Met and a mild phenotype have been described [28]. More recently, *de novo* missense mutations have been found in infantile onset spinocerbellar ataxia (encoding c.800C>G; p.Thr267Arg, c. 800C>T; p.Thr267Met, c.830G>T; p.Ser277Ile, c.1736C>T; p.Thr579Ile) [29] and ataxic cerebral palsy (encoding c.1759A>G; p.Asn587Asp, c.4459_4460delinsGA; p.Ser1487Asp) [30]. In total, eight intragenic mutations, substituting

seven residues, have been identified in 12 unrelated cases of cerebellar ataxia, with only one of these cases having an adult onset phenotype (Figure 2). It is notable that the more severe and earlier onset *ITPR1*-associated ataxia is caused predominantly by missense variants and that these missense variants are distinct from those associated with Gillespie syndrome. When trying to understand the molecular origins of the dominant phenotype, it is interesting to note that a dominant-negative effect has been described for mutations in several other transmembrane channel genes [31-33]. Thus we can hypothesize that a similar mechanism may account for the effects of the mutations identified here. Given that the ITPR1 protein forms a homotetramer (Fig. 2B), then only 1/16 assembled tetramers will contain four wildtype subunits, in the absence of any cotranslational assembly [34]. If a single mutated subunit can block channel function, then 94% of tetramers will be non-functional, thus potentially explaining the dominant phenotype.

We were unaware of any methods for predicting whether protein-altering mutations are likely to show a dominant-negative effect and we speculated that such variants should generally be less structurally perturbing than other LOF pathogenic mutations, because a dominant-negative mechanism requires the complex to, at least, partially assemble. To address this, we predicted the structural destabilization [35] of pathogenic missense mutations with a known or likely dominant-negative mechanism from proteins that form transmembrane channels, and compared them to recessive mutations from the same proteins or dominant mutations from genes with no known dominant-negative effect (Figure S1). We observe a highly significant difference ($p \leq 0.0015$) with the dominant-negative mutations inducing a lesser change in protein stability than the two other groups of mutations.

Next, using the recently determined cryoelectron microscopy structure of the tetrameric ITPR1 protein [36], we predicted the effects of the missense mutations identified in this study, as well as the cerebellar ataxia-associated missense mutations mentioned above. All but one of the *ITPR1* mutations are predicted to have mildly destabilising effects (Table S1). We compared these mutations to a larger set of known dominant-negative mutations in transmembrane channels, recessive mutations in the same transmembrane channels, and other dominant mutations with no known dominant-negative association (Figure S1). We observe that the dominant-negative mutations are significantly less destabilising than the

other groups. The pathogenic missense mutations in *ITPR* were found to be most similar to known dominant-negative mutations using these parameters. Only p.Gly2539Arg is predicted to be strongly destabilizing, although it is still within the range of some of the other known dominant-negative mutations. Additional evidence for the pathogenicity of p.Gly2539Arg comes from its position immediately N-terminal to the ion selectivity filter of the ITPR1 protein [37]. Indeed, site directed mutagenesis of p.Gly2539 to alanine has demonstrated a loss of channel activity in a number of *in vitro* assays [38]. Overall, this analysis strongly supports a dominant-negative mechanism for the mutations identified here, as has been observed in other transmembrane channels.

We can also consider how the different *ITPR1* mutations are located with respect to the three-dimensional structure of the complex (Fig. 2B). Interestingly, all three residues mutated in Gillespie syndrome are located near the centre of the channel, within or close to the transmembrane region, whereas all of the non-Gillespie mutations occur away from the centre within the cytoplasmic domains. Notably, 4/6 non-Gillespie positions are located at or near the $IP_3$ binding site [36]. The only point mutation associated with adult-onset *ITPR1*-associated ataxia (encoding p.Pro1068Leu) is located relatively near in space to another early-onset mutation, and is also predicted to be only mildly destabilizing, suggesting that it may also be associated with a dominant-negative mechanism, rather than the haploinsufficiency associated with SCA15 gene deletions.

The dominant negative hypothesis requires the mutant protein to be translated, stable and correctly targeted. To assess this we used lymphoblastoid cell lines (LCL) that had been established from five of the affected individuals with Gillespie syndrome. Two of these individuals carried c.7615G>A p.Gly2539Arg (2021_2021, 2018_2018) and three had c.7786_7788delAAG p.Lys2596del (291_291, 2374_2374, 1388_1388). Western blot of protein extracted from unsynchronized cultures revealed a variable level of ITPR1 between control and mutant LCL with no obvious difference between the groups (data not shown). Protein localization was assessed using immunofluorescence staining with confocal microscopy or structured illumination microscopy (SIM). As expected punctate perinuclear staining was seen in both control and mutant cell lines consistent with known localization to the smooth endoplasmic reticulum [39, 40](Figure 3A). ITPR1 is also known to localize to

structures within the nucleus known as the nucleoplasmic reticulum [41, 42]. In the Gillespie syndrome LCLs the most striking difference compared to control LCLs was a consistently higher proportion of cells that were positive ITPR1 using immunofluorescence (Figure 3B). Using quantitative analysis of super-resolution SIM images no significant differences could be detected in the number of fluorescence foci or the total volume of the ITPR1-positive regions within the whole cell or the nucleus (Figure 3C, S3). The irregularities in the nuclear outline in the mutant cells may be indicative of an increased number and/or increased size of the nucleoplasmic reticular pores (see Figure 4 in [42]). These changes may reflect failure of a feedback loop caused by a deficit in calcium signaling within the nucleus. However, we were unable to directly assess ITPR1-associated calcium signaling in the LCLs using ATP as no stimulation of calcium signaling was seen in either control or mutant cells (Figure S4).

Heterozygous null, non-mosaic, 16.5 dpc mouse embryos and adult mice were created using CRISPR/Cas9 genome editing methodology (Supplementary Information). These embryos displayed no obvious morphological differences in the early development of the iris compared to their wild type littermates (Figure S2A). Immunohistochemistry (IHC) of the wild type mouse embryos revealed no evidence of specific staining of ITPR1 in the developing iris (data not shown). No change in expression of Pax6 could be detected between mutant and wild type embryos (Figure S2A). Two heterozygous null adult mice could be examined at the age of 76 days with wild type littermate controls (Figure S2B). Although minor defects in the iris were noted in both mice no major anomalies that would be consistent with the phenotype seen in Gillespie Syndrome could be detected. These data suggest that the role of ITPR1 in iris development is either indirect, acting at a later stage of development or is tolerant of 50% residual channel activity. The latter explanation would be consistent with the lack of an iris phenotype in individuals affected with SCA15 in whom haploinsufficiency for *ITPR1* is the predominant genetic mechanism. Of note, $Ca^{2+}$ has been implicated in development of the eye in both chick and zebrafish, although the source of these ions has been thought to be extracellular (as reviewed in [43]).

The data presented here provide strong evidence that Gillespie syndrome is a clinically- and neuroradiologically- distinct disorder that shows locus homogeneity. The cerebellar anomalies in these cases are similar to that seen in the SCA29 phenotype. We

present evidence based on the predicted effect of mutations on the formation of multimeric channels that suggests that these mutations are likely to be acting by a dominant negative effect. This protein structure based analysis is likely to have wide applicability in the interpretation of mutations, particularly in the important "channelopathy" class of human disease genes [44-46]. The iris hypoplasia, which typifies Gillespie syndrome, may be a consequence of lower level of residual function in ITPR1 (compared to SCA29) but, given that only specific residues are altered, it seems more likely that these mutations disrupt functional interactions that are critical to the formation and/or maintenance of the sphincter pupillae muscle. In this regard it is interesting that mutations in the gene encoding a smooth muscle actin (*ACTA2,* MIM 102620) have recently been reported with a very similar iris phenotype [47]. ITPR1 and ATCT2 may interact in smooth muscle as components of the cGMP kinase signaling complex [48].

## Description of Supplemental Data

Figure S1: Predicted changes in protein stability

Figure S2: Phenotype of heterozygous null *Itpr1* mice

Figure S3: Super-resolution image quantification of ITPR1

Figure S4: Calcium release in *ITPR1* mutant cell lines

Table S1: FoldX predicted protein stability for *ITPR1* mutations

Table S2: Oligonucleotides used for *ITPR1*/*Itpr1* targeted sequencing

Table S3: Predicted pathogenicity scores for *ITPR1* mutations

## Acknowledgements

The DDD study presents independent research commissioned by the Health Innovation Challenge Fund [grant number HICF-1009-003], a parallel funding partnership between the Wellcome Trust and the Department of Health, and the Wellcome Trust Sanger Institute [grant number WT098051]. The views expressed in this publication are those of the author(s)

and not necessarily those of the Wellcome Trust or the Department of Health. The research team acknowledges the support of the National Institute for Health Research, through the Comprehensive Clinical Research Network. AHN is funded by Action Medical Research and The Henry Smith Charity. KAW, AS, JKR, JR, EF, AW, LMcK, AR, VvH, and DRF are funded by a program grant as part of the Medical Research Council (UK) grant to the University of Edinburgh for the MRC Human Genetics Unit. JAM is supported by a Medical Research Council Career Development Award (MR/M02122X/1). HB and MH are funded by grants from NewLife (14-15/07 and 13-14/02, respectively). The authors declare no conflict of interest related to this paper.

## Web Resources

Online Mendelian Inheritance in Man (http://www.omim.org)

Deciphering Developmental Disorders (www.ddduk.org)

Exome Aggregation Consortium (http://exac.broadinstitute.org/)

Ensembl (http://www.ensembl.org/)

National Center for Biotechnology Information (http://www.ncbi.nlm.nih.gov/)

DECIPHER database (decipher.sanger.ac.uk)

PolyPhen2 (http://genetics.bwh.harvard.edu 8 Feb 2016)

SIFT (http://grch37.ensembl.org/Homo_sapiens/Tools/VEP/ 8 Feb 2016)

MutationTaster (http://www.mutationtaster.org 8 Feb 2016)

Align GVGD (http://agvgd.iarc.fr/agvgd 8 Feb 2016)

European Genome-Phenome Archive (https://www.ebi.ac.uk/ega/home )

## Note added in proof

Gillespie syndrome Individual 1388_1388 described in this study is the same individual as F4:II2 who is described, with the same *ITPR1* mutation, in the accompanying report by Gerber *et al.* Biallelic truncating and *de novo* missense *ITPR1* mutations cause Gillespie syndrome.

# Figure Legends

## Figure 1: Human Genetic, Ophthalmic and radiological features of Gillespie syndrome

A. Diagrammatic representation of the Sanger sequencing chromatograms in 12 families in this study with a confident clinical diagnosis of Gillespie syndrome. In 9/12 *de novo* status of the mutations could be confirmed and in one family (SVP_SW) the mutation was inherited from an affected mother. B. Left panel: Image of the right eyes from 263220 and 5284_5284 showing iris hypoplasia and iridolenticular strands (arrowed) typical of Gillespie syndrome. Middle panel: MR brain imaging of 261348 at the age of 1 year and 7 months showing minor prominence of the cerebellar folia of the vermis superiorly but by 4 years 8 months progressive cerebellar vermian volume loss and minor prominence of the superior cerebellar folia of both cerebellar hemispheres. Minor periventricular high T2/FLAIR signal adjacent to frontal and occipital horns (white arrowheads). Right panel. MR brain imaging of 5285_5285 aged 11years 7months showing moderate vermis and cerebellar hemisphere atrophy, more prominent superiorly and in the vermis with minor increased periventricular white matter T2 signal adjacent to the frontal horns as well as a couple of foci within the frontal lobe white matter bilaterally(white arrowheads). C. Left panel: Right eye of 1388_1388 showing iris hypoplasia. Right panel: Individual 272179 at age 37 years. MR brain showing moderate vermis and cerebellar atrophy, worse in the vermis and superiorly. Abnormal periventricular increased T2/FLAIR signal adjacent to the frontal horns (white arrowheads). D. A photo of the right eye of 91_91 at age 52 years (*de novo* c.6280G>C p.Glu2094Gln) showing iris hypoplasia with fixed mydriasis. The adjacent MR imaging shows mild cerebellar volume loss (cerebellar hemispheres and vermis), more so superiorly. There is periventricular increased T2/FLAIR signal, most notably adjacent to the frontal horns with multiple foci of white matter increased T2/FLAIR signal elsewhere in the white matter mainly of the centrum semiovale. There is a minor degree of generalised cerebral atrophy. Gyral pattern appears normal.

## Figure 2: De novo mutations affecting three residues in ITPR1 are the major cause of Gillespie syndrome

A. Linear representation of ITPR1. Amino acid numbering is based on NP_001161744.1 (Q14643-2; ENSP00000306253.8) which has 2743 residues (encoded by the canonical transcript NM_001168272.1; ENST00000302640). The coloured boxes represent the following domains and features: green, ligand transferase domain; red, inositol 1,4,5 triphosphate binding domain; yellow, 15 amino acid insertion in isoform Q14643-1 (which has 2758 residues); brown RyR and IP3R homology domain; orange, intracellular transmembrane domain; blue, calcium ion transport channel. The heterozygous mutations associated with congenital cerebellar ataxia (blue text) mostly cluster towards the N-terminus at the ligand transferase and inositol 1,4,5 triphosphate binding domains, whereas those associated with autosomal dominant Gillespie syndrome (pink text) cluster towards the C-terminus at or near the intracellular transmembrane domain and calcium ion transport channel.

B. Structure of the ITPR1 tetramer, left, and monomer, right (derived from PDB ID: 3JAV). The three mutation sites from this study associated with Gillespie syndrome shown in red, and six sites previously associated with other disorders shown in blue.

## Figure 3: Functional characterization of ITPR1/Itpr1 mutations

Confocal imaging of lymphoblastoid cell lines (LCL) showing representative examples from unaffected individuals (control 1 as an exemplar) or individuals with Gillespie syndrome (291_291 and 2018_2018 as exemplars). The top panel shows DAPI stained nuclei. The panel below shows the punctate staining in the nuclear and perinuclear regions on immunofluorescence staining using an anti-ITPR1 antibody. *ITPR1* mutant cells consistently showed more punctate staining within the nucleus compared to the controls. The third panel shows the merge of the first and second. The fourth panel shows super-resolution SIM imaging of representative LCL nuclei from each of the genotypes, B. The number of ITPR1-stain positive cells in LCLs with or without mutations in *ITPR1* were analysed using ImageJ. Area, shape descriptor and mean gray value were measured for each cell. In control LCLs <20% of the DAPI positive (+ve) cells were also +ve for ITPR1 immunofluorescence. In cells carrying either of the indicated mutations, 30-50% of the cells were ITPR1 positive. Chi squared tests of the difference between the mutant and control cells suggest these are very unlikely to be chance observations. C. Quantitative fluorescence analysis from 3D super-resolution images showing the mean total volume of ITPR1-positive foci for the following compartments within the cell: whole cell, reticular component, whole nucleus and low-DAPI regions of the nucleus. Multiple individual cells from two independent patient-derived LCLs per genotype were obtained using Structured Illumination Microscopy (SIM). The masking strategy used to obtain these data is outlined in Figure S3. No significant difference was observed between genotypes.

Table 1: Summary of the clinical and molecular finding in individuals with Gillespie syndrome

| **Residue Involved** | Glu2094 | | | Gly2539 | | | | | | Lys2596 | | | |
|---|---|---|---|---|---|---|---|---|---|---|---|---|---|
| **Patient ID** | **91_91** | **SVP** | **SW** | **261348** | **263220** | **2021_2021** | **2018_2018** | **5284_5284** | **5285_5285** | **272179** | **291_291** | **2374_2374** | **1388_1388** |
| Genomic mutation hg19 | chr3 g.4821267G>C | chr3 g.4821268A>G | | chr3 g.4856205G>C | chr3 g.4856205G>A | chr3 g.4856205G>A | chr3 g.4856205G>A | chr3 g.4856205G>A | chr3 g.4856205G>A | chr3 g.4856866-4856868delAAG | chr3 g.4856866-4856868delAAG | chr3 g.4856866-4856868delAAG | chr3 g.4856866-4856868delAAG |
| Genotype | Het | Het | | Het | Het | Het | Het | Het | Het | Het | Het | Het | Het |
| Mutation Type | missense_variant | missense_variant | | missense_variant | missense_variant | missense_variant | missense_variant | missense_variant | missense_variant | inframe_deletion | inframe_deletion | inframe_deletion | inframe_deletion |
| NM_001168272.1; ENST00000302640 | c.6280G>C | c.6281A>G | | c.7615G>C | c.7615G>A | c.7615G>A | c.7615G>A | c.7615G>A | c.7615G>A | c.7786_7788delAAG | c.7786_7788delAAG | c.7786_7788delAAG | c.7786_7788delAAG |
| NP_001161744.1; ENSP00000306253.8 consequence | p.(Glu2094Gln) | p.(Glu2094Gly) | | p.(Gly2539Arg) | p.(Gly2539Arg) | p.(Gly2539Arg) | p.(Gly2539Arg) | p.(Gly2539Arg) | p.(Gly2539Arg) | p.(Lys2596del) | p.(Lys2596del) | p.(Lys2596del) | p.(Lys2596del) |
| *De novo* mutation | Yes | NK | Mat | Yes | Yes | Yes | NK | Yes | Yes | Yes | Yes | Yes | Yes |
| Sex | Female | Female | Female | Male | Female | Female | Female | Female | Male | Male | Female | Female | Female |
| Prenatal Growth | | | | | | | | | | | | | |
| Gestation | NK | NK | NK | 40 | 40 | 40 | NK | 40 | NK | 37 | 40 | 40 | 37 |
| Birth weight (SD) | NK | NK | "Normal" | 0.76 | 1.09 | 0.99 | NK | -1.17 | NK | 1.25 | -1.17 | -0.75 | 0.04 |
| Postnatal Growth | | | | | | | | | | | | | |
| Age (yearr) | 55 | 34 | 13 | 7.19 | 14.62 | 28 | NK | 3.4 | 12 | 36.95 | 10 | 16 | 19.75 |
| Height_SD | 0.53 | NK | NK | -0.38 | NK | NK | NK | -3.12 | NK | NK | -3 | -4.2 | 1 |
| Weight_SD | -2.31 | NK | NK | 0.19 | NK | NK | NK | -1.7 | NK | NK | -2 | NK | 1.8 |
| OFC_SD | 0.35 | NK | NK | -0.89 | 60.7 | NK | NK | -0.58 | NK | 2.39 | NK | NK | 2 |
| Neurology and development | | | | | | | | | | | | | |
| Sat independently | Late | NK | NK | 2 years | 2-2.5 years | 13 months | NK | 9 months | NK | Late | 18 months | 3 years | 30 months |
| Walked independently | 8-9 years | NK | NK | 10 years | Not yet achieved | >6 years | NK | Not yet achieved | NK | 10 years | Not yet achieved. | >10 years | 7 years |
| Speech delay | Yes | NK | NK | Severe | Yes | Moderate | NK | NK | NK | Moderate-severe | Yes | Yes | Yes |
| Intellectual disability | Mild to moderate | Learning difficulties | Mild | Learning difficulties | Mild | Mild to moderate | NK | Mild | Moderate | Mild-moderate | Global delay | Global delay | Mild |
| Hypotonia | NK | NK | Yes | No | Yes | Yes | NK | Yes | Yes | Yes | Yes | Yes | Yes, severe |
| Ataxia | Yes | Yes | Yes | Yes | Yes | Yes | Yes | Yes | Yes | Yes | Yes | Yes | Yes, severe |
| Cerebellar hypoplasia/atrophy | Yes | Yes | Yes | Yes | Yes | Yes | NK | Yes | Yes | Yes | Yes | Yes | Yes |
| Ophthalmology | | | | | | | | | | | | | |
| Bilateral Iris hypoplasia | Yes | Yes | Yes | Yes | Yes | Yes | Yes | Yes | Yes | Yes | Yes | Yes | Yes |
| Foveal hypoplasia | No | NK | NK | NK | Yes | NK | NK | NK | NK | No | NK | No | No |
| Visual impairment | Mild | NK | NK | NK | Mild | NK | NK | Mild | NK | NK | Mild | Moderate | NK |
| Negative *PAX6* screen | Yes | Exome | Exome | Yes | Yes | Yes | Yes | No | No | Yes | Yes | Yes | Yes |
| Clinical Diagnosis of Gillespie syndrome | Yes | Yes | Yes | Yes | Yes | Yes | Yes | Yes | Yes | Yes | Yes | Yes | Yes |
| Other Features | | | | | | | | | | | | | |
| Other Clinical Features | Gastrooesophageal reflux, depression | None | None | Gastroesophageal reflux | Scoliosis, gall stones | None | None | Patent foramen ovale and a mild pulmonary valve stenosis | None | Scoliosis, macrocephaly, small ears | None | Frontal bossing | slight facial dysmorphism |

NK: not known. Het: heterozygous variant. SD: Standard Deviation. OFC: occipito-frontal circumference

# References:


1. Mann IC. THE DEVELOPMENT OF THE HUMAN IRIS. Br J Ophthalmol, 9 (1925), 495-512.
2. Hingorani M, Hanson I, van Heyningen V. Aniridia. Eur J Hum Genet, 20 (2012), 1011-1017.
3. Netland PA, Scott ML, Boyle JWt, Lauderdale JD. Ocular and systemic findings in a survey of aniridia subjects. J AAPOS, 15 (2011), 562-566.
4. Sisodiya SM, Free SL, Williamson KA et al. PAX6 haploinsufficiency causes cerebral malformation and olfactory dysfunction in humans. Nat Genet, 28 (2001), 214-216.
5. Ito YA, Footz TK, Berry FB et al. Severe molecular defects of a novel FOXC1 W152G mutation result in aniridia. Invest Ophthalmol Vis Sci, 50 (2009), 3573-3579.
6. Sadagopan KA, Liu GT, Capasso JE, Wuthisiri W, Keep RB, Levin AV. Anirdia-like phenotype caused by 6p25 dosage aberrations. Am J Med Genet A, 167A (2015), 524-528.
7. Khan AO, Aldahmesh MA, Alkuraya FS. Genetic and genomic analysis of classic aniridia in Saudi Arabia. Mol Vis, 17 (2011), 708-714.
8. Chang TC, Summers CG, Schimmenti LA, Grajewski AL. Axenfeld-Rieger syndrome: new perspectives. Br J Ophthalmol, 96 (2012), 318-322.
9. van Heyningen V, Boyd PA, Seawright A et al. Molecular analysis of chromosome 11 deletions in aniridia-Wilms tumor syndrome. Proc Natl Acad Sci U S A, 82 (1985), 8592-8596.
10. Francois J, Lentini F, de Rouck F. Gillespie's syndrome (incomplete aniridia, cerebellar ataxia and oligophrenia). Ophthalmic Paediatr Genet, 4 (1984), 29-32.
11. Crawfurd MD, Harcourt RB, Shaw PA. Non-progressive cerebellar ataxia, aplasia of pupillary zone of iris, and mental subnormality (Gillespie's syndrome) affecting 3 members of a non-consanguineous family in 2 generations. J Med Genet, 16 (1979), 373-378.
12. Ansari M, Rainger J, Hanson IM et al. Extended Mutation Analysis in PAX6-Negative Aniridia/Iris Hypoplasia. PLoS ONE, Submitted.
13. Firth HV, Wright CF. The Deciphering Developmental Disorders (DDD) study. Dev Med Child Neurol, 53 (2011), 702-703.
14. Large-scale discovery of novel genetic causes of developmental disorders. Nature, 519 (2015), 223-228.
15. Akawi N, McRae J, Ansari M et al. Discovery of four recessive developmental disorders using probabilistic genotype and phenotype matching among 4,125 families. Nat Genet, 47 (2015), 1363-1369.
16. Wright CF, Fitzgerald TW, Jones WD et al. Genetic diagnosis of developmental disorders in the DDD study: a scalable analysis of genome-wide research data. Lancet, 385 (2015), 1305-1314.
17. Ramu A, Noordam MJ, Schwartz RS et al. DeNovoGear: de novo indel and point mutation discovery and phasing. Nat Methods, 10 (2013), 985-987.
18. Cunningham F, Amode MR, Barrell D et al. Ensembl 2015. Nucleic Acids Res, 43 (2015), D662-9.
19. Marien P, Brouns R, Engelborghs S et al. Cerebellar cognitive affective syndrome without global mental retardation in two relatives with Gillespie syndrome. Cortex, 44 (2008), 54-67.

20. Verhulst S, Smet H, Ceulemans B, Geerts Y, Tassignon MJ. Gillespie syndrome, partial aniridia, cerebellar ataxia and mental retardation in mother and daughter. Bull Soc Belge Ophtalmol, 250 (1993), 37-42.
21. Di Gregorio E, Orsi L, Godani M et al. Two Italian families with ITPR1 gene deletion presenting a broader phenotype of SCA15. Cerebellum, 9 (2010), 115-123.
22. Ganesamoorthy D, Bruno DL, Schoumans J et al. Development of a multiplex ligation-dependent probe amplification assay for diagnosis and estimation of the frequency of spinocerebellar ataxia type 15. Clin Chem, 55 (2009), 1415-1418.
23. Marelli C, van de Leemput J, Johnson JO et al. SCA15 due to large ITPR1 deletions in a cohort of 333 white families with dominant ataxia. Arch Neurol, 68 (2011), 637-643.
24. Novak MJ, Sweeney MG, Li A et al. An ITPR1 gene deletion causes spinocerebellar ataxia 15/16: a genetic, clinical and radiological description. Mov Disord, 25 (2010), 2176-2182.
25. Obayashi M, Ishikawa K, Izumi Y et al. Prevalence of inositol 1, 4, 5-triphosphate receptor type 1 gene deletion, the mutation for spinocerebellar ataxia type 15, in Japan screened by gene dosage. J Hum Genet, 57 (2012), 202-206.
26. Synofzik M, Beetz C, Bauer C et al. Spinocerebellar ataxia type 15: diagnostic assessment, frequency, and phenotypic features. J Med Genet, 48 (2011), 407-412.
27. Huang L, Chardon JW, Carter MT et al. Missense mutations in ITPR1 cause autosomal dominant congenital nonprogressive spinocerebellar ataxia. Orphanet J Rare Dis, 7 (2012), 67.
28. Shadrina MI, Shulskaya MV, Klyushnikov SA et al. ITPR1 gene p.Val1553Met mutation in Russian family with mild Spinocerebellar ataxia. Cerebellum Ataxias, 3 (2016), 2.
29. Sasaki M, Ohba C, Iai M et al. Sporadic infantile-onset spinocerebellar ataxia caused by missense mutations of the inositol 1,4,5-triphosphate receptor type 1 gene. J Neurol, 262 (2015), 1278-1284.
30. Parolin Schnekenberg R, Perkins EM, Miller JW et al. De novo point mutations in patients diagnosed with ataxic cerebral palsy. Brain, 138 (2015), 1817-1832.
31. Kubisch C, Schroeder BC, Friedrich T et al. KCNQ4, a novel potassium channel expressed in sensory outer hair cells, is mutated in dominant deafness. Cell, 96 (1999), 437-446.
32. Mulders SM, Bichet DG, Rijss JP et al. An aquaporin-2 water channel mutant which causes autosomal dominant nephrogenic diabetes insipidus is retained in the Golgi complex. J Clin Invest, 102 (1998), 57-66.
33. Yeromin AV, Zhang SL, Jiang W, Yu Y, Safrina O, Cahalan MD. Molecular identification of the CRAC channel by altered ion selectivity in a mutant of Orai. Nature, 443 (2006), 226-229.
34. Wells JN, Bergendahl LT, Marsh JA. Co-translational assembly of protein complexes. Biochem Soc Trans, *43* 10.1042/BST20150159.
35. Guerois R, Nielsen JE, Serrano L. Predicting changes in the stability of proteins and protein complexes: a study of more than 1000 mutations. J Mol Biol, 320 (2002), 369-387.
36. Fan G, Baker ML, Wang Z et al. Gating machinery of InsPR channels revealed by electron cryomicroscopy. Nature, (2015),
37. Dellis O, Dedos SG, Tovey SC, Taufiq-Ur-Rahman Dubel SJ, Taylor CW. Ca2+ entry through plasma membrane IP3 receptors. Science, 313 (2006), 229-233.

38. Schug ZT, da Fonseca PC, Bhanumathy CD et al. Molecular characterization of the inositol 1,4,5-trisphosphate receptor pore-forming segment. J Biol Chem, 283 (2008), 2939-2948.
39. Mikoshiba K, Furuichi T, Miyawaki A et al. The inositol 1,4,5-trisphosphate receptor. CIBA Found Symp, 164 (1992), 17-29; discussion 29-35.
40. Taylor CW, Richardson A. Structure and function of inositol trisphosphate receptors. Pharmacol Ther, 51 (1991), 97-137.
41. Echevarria W, Leite MF, Guerra MT, Zipfel WR, Nathanson MH. Regulation of calcium signals in the nucleus by a nucleoplasmic reticulum. Nat Cell Biol, 5 (2003), 440-446.
42. Lui PP, Chan FL, Suen YK, Kwok TT, Kong SK. The nucleus of HeLa cells contains tubular structures for Ca2+ signaling with the involvement of mitochondria. Biochem Biophys Res Commun, 308 (2003), 826-833.
43. Webb SE, Miller AL. Calcium signalling during embryonic development. Nat Rev Mol Cell Biol, 4 (2003), 539-551.
44. Bennett DL, Woods CG. Painful and painless channelopathies. Lancet Neurol, 13 (2014), 587-599.
45. Statland J, Phillips L, Trivedi JR. Muscle channelopathies. Neurol Clin, 32 (2014), 801-15, x.
46. Webster G, Berul CI. An update on channelopathies: from mechanisms to management. Circulation, 127 (2013), 126-140.
47. Roulez FM, Faes F, Delbeke P et al. Congenital fixed dilated pupils due to ACTA2- multisystemic smooth muscle dysfunction syndrome. J Neuroophthalmol, 34 (2014), 137-143.
48. Koller A, Schlossmann J, Ashman K, Uttenweiler-Joseph S, Ruth P, Hofmann F. Association of phospholamban with a cGMP kinase signaling complex. Biochem Biophys Res Commun, 300 (2003), 155-160.

Figure 1



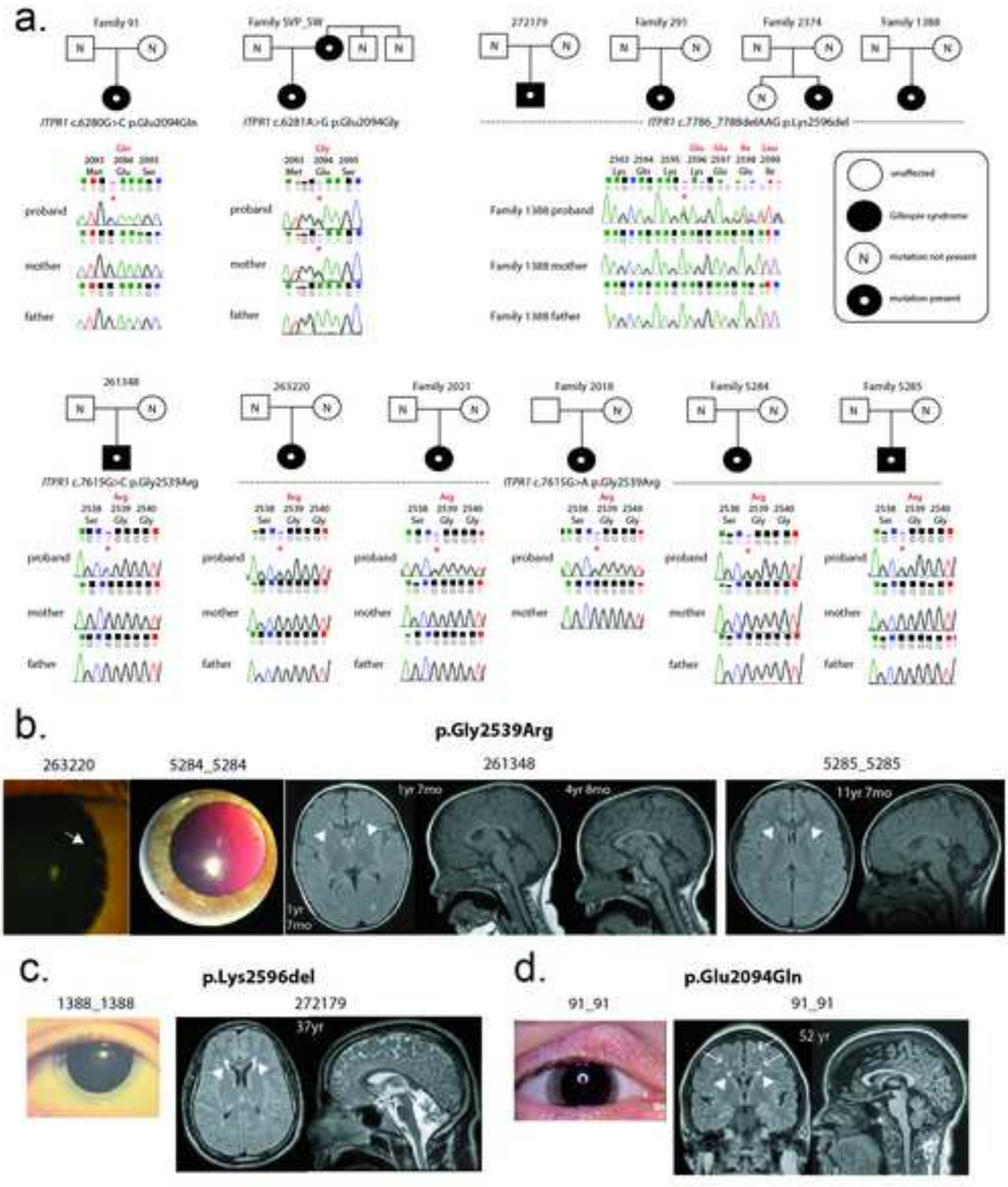

Figure 2



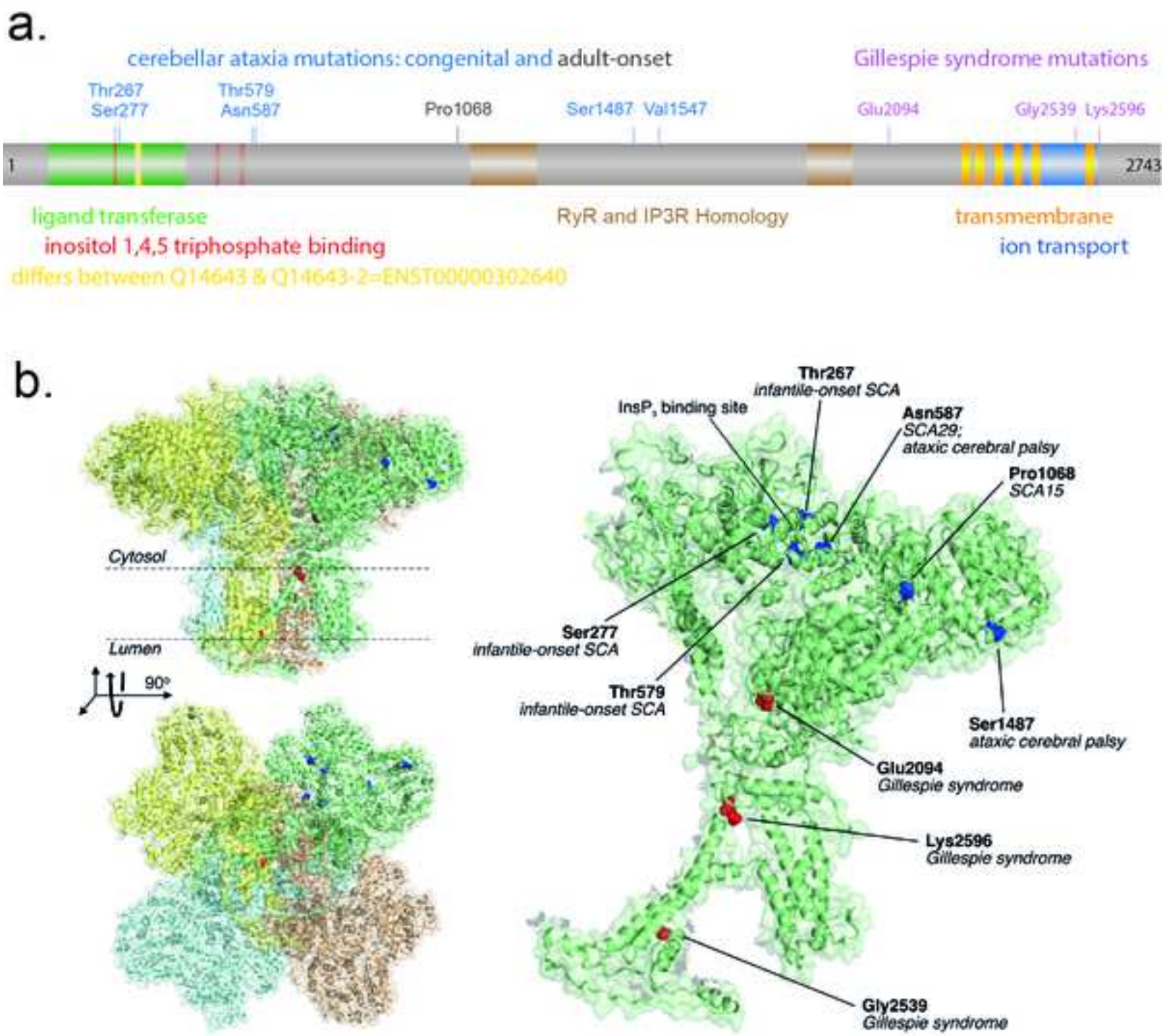

Figure 3

Click here to download Figure Itpr1 Final Figure 3.tif